Simulating the Role of Microtubules in Depolymerization-Driven Transport: A Monte Carlo Approach

Yong-Chuan Tao* and Charles S. Peskin#
*Department of Physics, New York University, New York, New York 10003 and #Courant Institute of Mathematical Sciences, New York University, New York, New York 10012 USA

ABSTRACT In this paper we present a model that simulates the role of microtubules in depolymerization-driven transport. The model simulates a system that consists of a 13-protofilament microtubule with "five-start" helical structure and a motor protein-coated bead that moves along one of the protofilaments of the microtubule, as in in vitro experiments. The microtubule is simulated using the lateral cap model, with substantial generalizations. For the new terminal configurations in the presence of the bead, rate constants for association and dissociation events of tubulin molecules are calculated by exploring the geometric similarities between different patterns of terminal configurations and by decomposing complex patterns into simpler patterns whose corresponding rate constants are known. In comparison with a previous model, in which simplifications are made about the structure of the microtubule and in which the microtubule can only depolymerize, the detailed structure of the microtubule is taken into account in the present model. Furthermore, the microtubule can be either polymerizing or depolymerizing. Force-velocity curves are obtained for both zero and non-zero tubulin guanosine 5′-triphosphate (GTP) concentrations. By analyzing the trajectory of the bead under different parameters, the condition for "run and pause" is analyzed, and the time scale of "run" and "pause" is found to be different for different motor proteins. We also suggest experiments that can be used to examine the results predicted by the model.

INTRODUCTION

Microtubules are long, stiff polymers made of tubulin; they are present in almost all eukaryotic cells and play important roles in many cellular processes, such as cell division and intracellular transport (Wade and Hyman, 1997; Hyams and Lloyd, 1994; Roberts and Hyams, 1979). During mitosis, microtubules form the mitotic spindle, which organizes chromosomes spatially and divides them between the two daughter cells (Inoué, 1981; Alberts et al., 1994; Rieder and Alexander, 1990). Many antimitotic drugs for cancer treatment, such as taxol, function by interfering with microtubule assembly or formation in cells. Because of its importance, better understanding of the roles of microtubules in intracellular transport and during mitosis has been the goal of experimentalists and theorists alike for many years.

A microtubule consists of tubulin heterodimers arranged in a helical structure. Typically, the heterodimers align along 13 different protofilaments that are parallel to the axis of the microtubule (Roberts and Hyams, 1979). Microtubules grow and shrink by association or dissociation of tubulin dimers at the ends. It is important to note that the two ends of a microtubule are different because of the polarity of the dimers. The "plus" end grows and shrinks faster than the "minus" end (Wade and Hyman, 1997; Alberts et al., 1994). In the cell, the minus end of a microtubule is generally embedded in a microtubule-organizing center, such as the poles of a mitotic spindle, whereas the plus end is often located near the plasma membrane (Alberts et al., 1994). During mitosis, the plus end may be connected to a chromosome at the kinetochore, and the minus end-directed motion of the chromosomes along the microtubules provides the traction mechanism for moving each of the two sister chromatids into one of the daughter cells (Alberts et al., 1994; Semënov, 1996).

Microtubules are extremely labile: they display the property of dynamic instability when the concentration of tubulin-GTP in the environment is near a critical level. In such an environment a microtubule alternates between the state of "catastrophe," when the microtubule shrinks quickly, and the state of "rescue," when the microtubule regains length. Many experiments have been performed to study dynamic instability (Mitchison and Kirschner, 1984; Walker et al., 1988; Mandelkow et al., 1991; Odde et al., 1995), and several models are available (Hill, 1984; Hill and Chen, 1984; Bayley et al., 1990; Martin et al., 1993; Dogterom and Leibler, 1993).

Two molecular processes underlie the roles of microtubules during mitosis, namely the change in the lengths of microtubules by polymerization and depolymerization, and the mechanochemical actions of motor proteins (Hyams and Lloyd, 1994; Koshland et al., 1988).

Motor proteins bind at one end to various cellular objects they are transporting and at the other end to the microtubule. There are basically two kinds of microtubule-associated motor proteins: plus motors, such as axonal kinesin, move toward the plus end of the microtubules; minus motors, such as cytoplasmic dyneins and a *Drosophila* kinesin called NCD, move toward the minus end of the microtubule (Alberts et al., 1994; Desai and Mitchison, 1995).

Received for publication 31 July 1997 and in final form 5 May 1998.

Address reprint requests to Prof. Charles S. Peskin, Courant Institute of Mathematical Sciences, New York University, 251 Mercer St., New York, NY 10012. Tel.: 212-998-3126; Fax: 212-995-4121; E-mail: peskin@cims.nyu.edu.

0006-3495/98/09/1529/12 $2.00

In vitro, chromosomes have been replaced by tiny beads coated with microtubule-associated motor proteins. Such a system is illustrated in Fig. 1. Experiments (Lombillo et al., 1995; Coue et al., 1991) have revealed a paradoxical picture: transportation of the bead toward the minus end of the microtubule by depolymerization at the plus end is enhanced in the presence of ATP, which fuels the motor action of the plus motor protein coated on the bead. Experiments have also shown that the motion of the bead is saltatory, with periods of runs and pauses.

A model was proposed by Peskin and Oster (1995) to explain these experimental results. The force-velocity curve obtained by using that model has a peak velocity: initially, when the load is smaller than the force that corresponds to the peak velocity, an increase in the plus end-directed force actually speeds up the minus end-directed transport of the bead. This result is consistent with the paradoxical phenomenon that has been observed in experiments. The model also predicts a saltatory trajectory of the bead, which is consistent with the run and pause characteristics observed in experiments.

The model presented by Peskin and Oster (1995) is based on several simplifications: first, the structure of the microtubule is simplified in that model. The model assumes that the basic building block of the microtubule is a circular ring that consists of 13 tubulin dimers, one from each protofilament. These rings are placed next to each other, and the resultant hollow cylinder is the microtubule. With such a model, the lengths of the 13 protofilaments in the microtubule are always the same, because when the microtubule depolymerizes; it is assumed that a whole ring of 13 dimers, one from each protofilament, comes off. In reality, polymerization and depolymerization are achieved by association or dissociation of individual tubulin dimers to or from the end of a protofilament. As a result, the end of the microtubule is almost always ragged. Furthermore, because the bead can catalyze the depolymerization of the protofilament on which it is moving, the length of that protofilament could be much shorter than those of the other protofilaments. Second, the model assumes that a stand-alone microtubule without anything attached to it would depolymerize at a constant rate. In reality, however, the depolymerization rate is not a constant of time due to the random nature of the depolymerization process. In general, the microtubule can grow or shrink and does so in a complicated way, involving the phenomena of dynamic instability as described above. Third, the model of Peskin and Oster (1995) deals only with the situation when [Tu-GTP], i.e., the concentration of tubulin-GTP, is zero. This eliminates the possibility that a protofilament can grow at times.

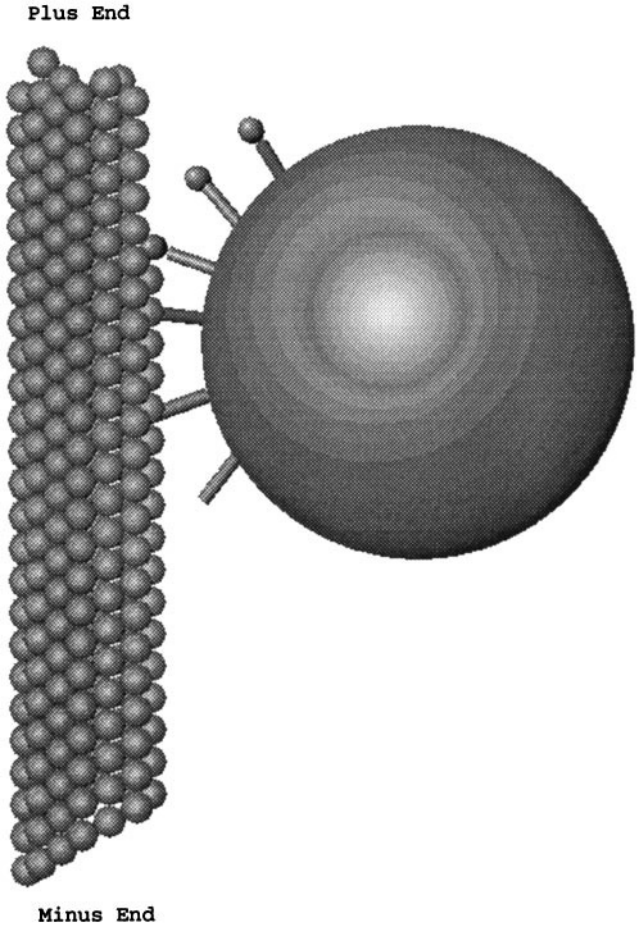

FIGURE 1 A latex bead is coupled to the microtubule by motor protein molecules. Notice that this figure is not drawn to scale. If it were, the bead would be much larger.

In this paper we extend the model of Peskin and Oster (1995) by presenting a more realistic model of the latex bead attached to a microtubule that may be polymerizing or depolymerizing at its plus end. Although more sophisticated microtubule models are available (Martin et al., 1993), for the purpose of this paper, in which the microtubule has a 13-protofilament A-lattice, we will simply use the lateral cap model of Bayley et al. (1990). The microtubule in our model has 13 protofilaments and a five-start helical structure. It incorporates a "lateral cap," which means that the tubulin dimer at the plus end of each protofilament may be in either of two states with different polymerization and depolymerization kinetics. The novel feature of the present paper is that we include a latex bead attached to the microtubule by motor protein molecules and the bead influences the dynamics of the system. This requires a substantial generalization of the Bayley model, since the bead generates many new terminal configurations that the microtubule cannot have when the bead is not present.

Simulations using the new model for the system generate a similar force-velocity curve as the one presented by Peskin and Oster (1995). The old and new models agree well at all loads, but especially at large load. This could be attributed to the fact that at very large load there is not much difference between the lengths of the protofilaments, and therefore the assumption of using rings as basic blocks for the microtubule is more reasonable. At small load, however, the new model shows that the length of the protofilament on which the bead moves can be much shorter than those of the other protofilaments; this difference is noticeable from the

force-velocity curves, but the difference is perhaps too small to allow experimental discrimination. Finally, under certain conditions, the trajectory of the bead produced by the new model exhibits the run and pause characteristic, which is in agreement with what has been observed in the model of Peskin and Oster (1995) and in experiments. Both the force-velocity curve and the time scales of the run and pause behaviors are different for different motor proteins, such as NK350 and kinesin. Such differences as predicted by the model could be examined in experiments.

THE MODEL

There are two major components in the system: the microtubule and the motor protein-coated bead that is attached to the microtubule.

The microtubule

For the purpose of this paper, the microtubule part of our model will be based on the lateral cap model presented in the paper of Bayley et al. (1990). However, because of the interaction between the latex bead and the microtubule, the lateral cap model needs to be substantially generalized.

Before we introduce the complete model for the microtubule with the bead attached, we will first briefly describe the lateral cap model for a stand-alone (without the bead) microtubule, as discussed in the paper of Bayley et al. (1990).

The dynamics of the microtubule simulated with a lateral cap model are determined by a single terminal layer of tubulin molecules. This model assumes that it is impossible for a tubulin molecule to dissociate from the microtubule when it is in the middle of a helix or a protofilament, where the affinity for the microtubule is strong. For example, in Fig. 2 *a*, the molecule in unit *b* cannot dissociate from the microtubule because it is in the middle of a protofilament,

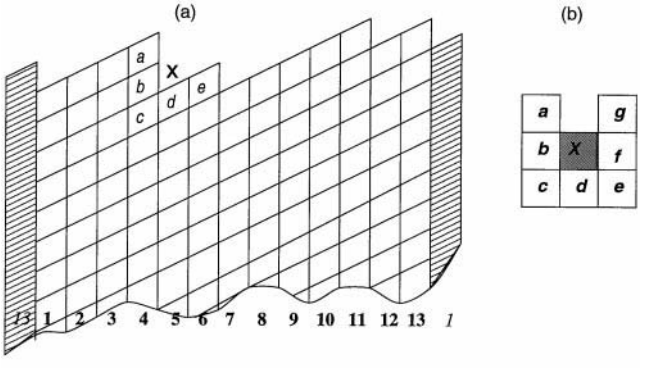

FIGURE 2 (*a*) The cylindrical projection of a 13-protofilament microtubule with five-start helical structure. The protofilaments are numbered from 1 to 13. Both 1 and 13 are each drawn twice to show that they are next to each other and to give a better picture of the helical structure. (*b*) For convenience, we use letters *a* through *g* to label the units surrounding a possible site X.

and the molecule in unit *d* cannot dissociate from the microtubule because it is in the middle of a helix. Therefore, a possible site for a dissociation event must be at the end of a helix and the end of a protofilament simultaneously. For example, in Fig. 2 *a*, it is possible for the molecule in unit *e* to dissociate from the microtubule.

Similarly, the criterion for a possible binding site is that at such a site, the incoming tubulin molecule will be at both the end of a helix and the end of a protofilament. For example, the vacant position *X* in Fig. 2 *a* is a possible binding site at which an incoming tubulin molecule can attach itself.

According to the criteria discussed above, a possible site, whether it is for association or dissociation, will be at the corner formed by two tubulin molecules, one of which interacts laterally with the incoming or the outgoing molecule, and the other accounts for the longitudinal interaction. For site *X* in Fig. 2 *a*, *b* and *d* are two such molecules. The rate constant for an association or a dissociation event at the site is determined primarily by what each of these two molecules is (tubulin-GDP or tubulin-GTP). Furthermore, we assume that apart from these two immediate neighbors of a site only the next-to-immediate neighbors (*a* and *e* for site *X*) will have contributions by modifying the rate constant by a certain factor. Therefore, an examination of the end of a protofilament in relation to its two adjacent protofilaments is enough to determine whether a site for association or dissociation exists at the end of that protofilament and the rate constant for an event at the site. In Fig. 2 *a*, the rate constant for an association event at the binding site *X* is determined primarily by what is in *b* and what is in *d*, with the molecules in *a* and *e* each contributing a factor of 2. Similarly, for a dissociation event, next-to-immediate neighbors will contribute a factor of ½ to the rate constants. Fig. 3 shows all possible configurations at the end of a protofilament of a stand-alone microtubule.

It is important to note the "hydrolysis rule" (Bayley et al., 1990): in the lateral cap model, tubulin-GTP molecules are confined to the terminal layer (lateral cap) of the microtubule. One way to determine whether a molecule is in the terminal layer is to check the number of its immediate neighbors (including diagonal neighbors). Usually, a molecule inside the microtubule has eight neighbors, but for one in the terminal layer, the number of neighbors is less than eight. Therefore, after an association event, tubulin-GTP molecules that are not in the terminal layer would hydrolyze and become tubulin-GDP molecules. For example, in Fig. 2 *a*, *a–e* are all in the terminal layer before the attachment at *X*. After the attachment, a tubulin-GTP molecule previously at site *c* will be hydrolyzed into a tubulin-GDP molecule.

When there is a bead moving along the microtubule, the terminal configurations can get much more complicated. As a result, the lateral cap model described above must be generalized: the assumption that a tubulin molecule cannot dissociate when it is in the middle of a helix does not apply here any more. This is because there is now a new depolymerization mechanism: when the bead is at the plus end and

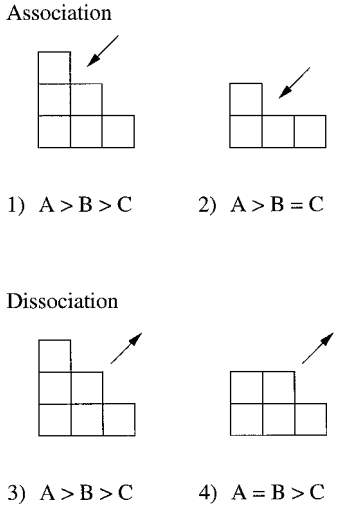

FIGURE 3 All possible terminal configurations for a stand-alone microtubule. In each case, the length of each protofilament from left to right is A, B, and C, respectively. The protofilament in the middle, i.e., the one with length B, is under consideration for possible sites of association or dissociation. Arrows indicate whether the site is for association or dissociation.

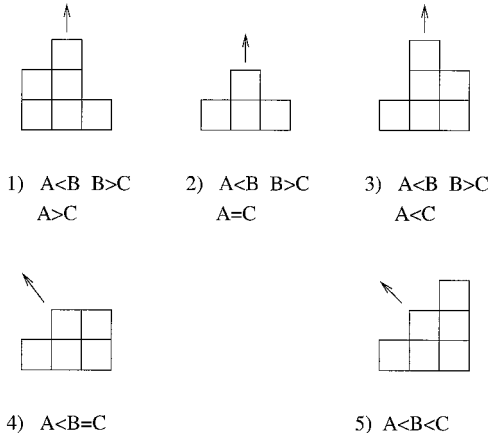

FIGURE 5 All possible dissociation sites in addition to those shown in Fig. 3 for a microtubule with a bead attached. The notations are the same as in Fig. 3.

rolls toward the minus end, the tubulin molecule at the plus end of the protofilament along which the bead is moving might be pulled off by the bead. This new depolymerization mechanism will lead to many new terminal configurations in addition to those configurations of a stand-alone microtubule. These new terminal configurations are illustrated in Figs. 4 and 5, with Fig. 4 showing all the possible sites for association and Fig. 5 showing all the possible sites for dissociation. Consequently, a new set of rate constants needs to be obtained for events that occur at these new terminals. The method to obtain the rate constants will be discussed in detail later in this paper.

The bead

Modeling the movement of the bead is relatively straightforward. We need only to keep track of the position of the bead in relation to the plus end of the protofilament along which the bead is moving. It turns out that only one variable is needed to describe the position of the bead. This is based upon the experimental evidence (Lombillo et al., 1995) that the movement of the bead is usually one-dimensional: the bead is traveling along one single protofilament, the displacement of the bead is always parallel to the microtubule axis, and there is no movement in the direction perpendicular to the microtubule axis. A detailed discussion of this issue can be found in the review by Howard (1995). Furthermore, we assume that the bead moves in steps of size δ, the length of a tubulin heterodimer, which is typically 8 nm. As discussed in the review by Howard (1995), for microtubules with different structures the step size might be different; it might even alternate between two different values for two consecutive walks in the same direction. In this paper, however, we will be content with a constant step size of 8 nm. It is not difficult to modify our model to accommodate different step sizes.

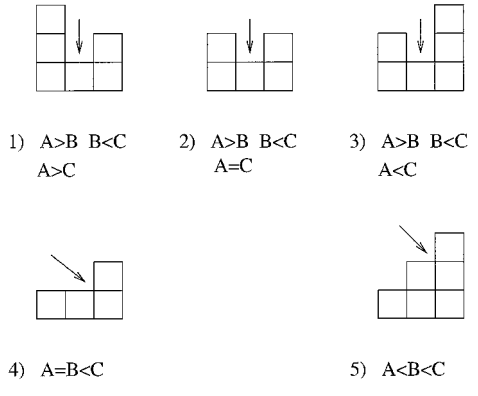

FIGURE 4 All possible association sites in addition to those shown in Fig. 3 for a microtubule with a bead attached. The notations are same as in Fig. 3.

Our model also assumes the following when the bead is located at the plus end the protofilament: first, the possibility for the bead to move further toward the plus end is zero, which means that the bead cannot fall off the microtubule. This assumption is reasonable only when the plus end-directed force applied on the bead is not extremely strong; otherwise, a separate process, namely the detachment of the bead from the microtubule, needs to be introduced. Second, if the bead is moving toward the minus end, it is possible that the bead can pull the terminal unit off. To simplify the problem, we assume that the possibility for the bead to pull off that unit is a constant, p_{off}. Of course, in reality one would expect that p_{off} would depend on the terminal configuration in a similar fashion, as in the cases for association and dissociation events. Such dependence will be studied in future work. Third, the molecule at the plus end of the protofilament along which the bead is moving cannot dissociate when the bead itself is at the plus end unless it is pulled off by the bead. This assumption is based upon the

consideration that the affinity for the bead makes it very difficult for that molecule to come off the microtubule unless it is pulled off by the bead when it moves.

One can also speculate that even if the bead is not at the end of the protofilament, it is still possible for the bead to pull off a molecule in the middle of the protofilament, thereby leaving holes in the microtubule (Semënov, 1996). However, it is reasonable to argue that the possibility for creating such holes is small, because a molecule in the middle of the microtubule is surrounded by other molecules and is therefore strongly bonded to the microtubule. Our model does not allow tubulin dimers in the middle of a protofilament to be pulled off by the bead.

The interplay between the movement of the bead and the polymerization and depolymerization of the microtubule makes the dynamics of the system extremely interesting: on one hand, because of the possibility of the bead pulling off the tubulin molecule at the plus end, many new patterns of terminal configurations are created; these new configurations give rise to new possibilities of polymerization and depolymerization that would otherwise not be present in a stand-alone microtubule. Furthermore, we assume that the tubulin molecule at the plus end of the protofilament to which the bead is attached cannot dissociate by itself if the bead is at the plus end. This would also have an effect on the dynamics of the microtubule by preventing certain dissociation events from taking place. On the other hand, depolymerization of the microtubule has an effect on the movement of the bead: it is assumed that the bead cannot fall off the microtubule. Therefore, when the bead is at the plus end, the possibility for it to move toward the plus end is zero. As a result, the movement of the bead is biased toward the minus end whenever the plus end of the protofilament along which the bead is moving catches up with the bead.

A Monte Carlo method is used in the simulation. There are three major kinds of events that might take place in the system: association of tubulin molecule to the microtubule, dissociation of tubulin molecule from the microtubule, and movement of the bead. Because of the stochastic nature of the system, the time interval between two consecutive events is random, and follows an exponential distribution. By repeatedly selecting an event and allowing it to occur, the dynamics of the system can be simulated. The rules for selecting the events will be discussed below.

SELECTION OF EVENTS

The simulation procedure will produce a sequence of events (association, dissociation, or walk of the bead). The dynamics of the system are obtained by monitoring the length of each protofilament of the microtubule as well as the position of the bead as a function of time. The Monte Carlo method is used to determine, on a probabilistic basis, which of the possible events is the first to take place and should be selected.

We first consider a stand-alone microtubule, with no bead attached. The simulation program examines the end of each protofilament for possible sites for association or dissociation, according to the criteria discussed above. There could be several possible sites of association or dissociation for a particular terminal configuration. The random time interval Δt_i at which an event associated with a site i would occur relative to the previous event follows an exponential distribution, which can be sampled as follows:

$$\Delta t_i = -\frac{\ln(1 - r_i)}{k_i}, \tag{1}$$

where k_i is the rate constant for the individual event at site i, and r_i is a random number uniformly distributed in [0,1), independent for different i.

The event that would occur the earliest is allowed to take place, and the time is advanced by Δt, which is given by the following equation:

$$\Delta t = \min\{\Delta t_i\}. \tag{2}$$

In the presence of the bead, the movement of the bead, either toward the plus end or the minus end, is also a possible event. If the rate constant for the bead to move toward the plus end is γ_+, then the time at which the bead could be moving toward the plus end, Δt_+, is given by

$$\Delta t_+ = -\frac{\ln(1 - r_+)}{\gamma_+}, \tag{3}$$

where r_+ is, as r_i, independently chosen from the uniform distribution on [0,1).

Similarly, if the rate constant for the bead to move toward the minus end is γ_-, then Δt_-, the time at which the bead could be moving toward the minus end, is given by

$$\Delta t_- = -\frac{\ln(1 - r_-)}{\gamma_-}, \tag{4}$$

where r_- is defined in the same way as r_+.

In summary, the next event that occurs is the one that corresponds the smallest of all Δt_i, Δt_+, and Δt_-, and the time is advanced by Δt, which is given by

$$\Delta t = \min\{\Delta t_i, \Delta t_+, \Delta t_-\}. \tag{5}$$

RATE CONSTANTS

Rate constants play key roles in determining the frequency of different kinds of events, and hence the dynamics of the system. However, the lack of understanding of the microscopic details of each process and the scarcity of experimental data make it difficult to determine an appropriate set of rate constants.

Rate constants for bead movement

At zero load it is assumed that it is equally possible for the bead to move toward either end of the microtubule, i.e., the rate constant for moving toward the plus end γ_+ is equal to

the rate constant for moving toward the minus end γ_-, unless the bead is at the end of the microtubule and a further step toward the end would cause it to fall off the microtubule. However, when the load is not zero, the movement of the bead is biased, and γ_+ and γ_- are different. If the force acting on the bead is f, then the relationship between γ_+ and γ_- can be determined by thermodynamics:

$$\gamma_+/\gamma_- = \exp(\xi), \tag{6}$$

where

$$\xi = f\delta/(k_B T), \tag{7}$$

k_B is the Boltzmann constant, T is the absolute temperature of the environment, and δ, as before, is the size of a single step, which is the same as the length of a tubulin heterodimer in our model.

Equation 6 gives only the ratio of γ_+ to γ_-; if one of them is known, the other can also be determined. We introduce a parameter γ, such that

$$\gamma_+ = \gamma \exp(\xi/2), \tag{8}$$

$$\gamma_- = \gamma \exp(-\xi/2). \tag{9}$$

Strictly speaking, γ could also be a function of ξ; however, for simplicity, we assume that γ is a constant. When the load is zero, it is obvious that $\gamma_+ = \gamma_- = \gamma$.

Rate constants for association and dissociation

For the association or dissociation events, the rate constants are far more difficult to determine. Again, we will start from a stand-alone microtubule as discussed in the paper of Bayley et al. (1990), and then make substantial generalizations to accommodate the new terminal configurations in the presence of the bead.

As mentioned above, the rate constant for an event at a site is determined predominantly by the two molecules that immediately surround the site. In Fig. 2 *a*, the principal part of the rate constant for an event at site X depends on what is in b and what is in d. Furthermore, to account for the roles of the next-to-immediate neighbors in the terminal layer, such as a and e for X in Fig. 2 *a*, we assume that they each contribute a factor of 2 (for association) or ½ (for dissociation) to the rate constants. For association, the rate constants will also depend proportionally on the concentration of tubulin-GTP in the environment.

For convenience, we use letters a through f to label the neighboring units of a site, as shown in Fig. 2 *b*. The basic set of rate constants, i.e., the rate constant for either an association or a dissociation event at site X, given the contents of units b and d, is adopted from the paper of Bayley et al. (1990), as shown in Table 1. $k(+T)$ stands for the rate constant of attaching a tubulin-GTP molecule to a vacant site at X, $k(-T)$ stands for the rate constant for a tubulin-GTP molecule at site X to dissociate from the microtubule, and so on. To take into account the effects of next-to-immediate neighbors of a site, $k(+T)$ is doubled for each molecule in a or e, and $k(-T)$ and $k(-D)$ are both halved for each molecule in a or e.

TABLE 1 Rate constants of association and dissociation events for the basic patterns of terminal configurations

Contents of sites b and d	$10^{-6} \times k(+T)_{bd}$ (M^{-1} s^{-1})	$k(-D)_{bd}$ (s^{-1})	$k(-T)_{bd}$ (s^{-1})
DD	0.33	111.66	66.66
DT, TD	1.00	—	8.33
TT	1.25	—	1.25

The basic set of rate constants for association and dissociation events, taken from Bayley et al. (1990). T stands for tubulin-GTP, D stands for tubulin-GDP. $k(+T)$ is the rate constant for adding a tubulin-GTP molecule to site X, at the corner formed by b and d (see Fig. 2), $k(-T)$ is the rate constant for a tubulin-GTP molecule at site X to dissociate, and so on. — stands for events that are not allowed.

As shown in Fig. 3, for a stand-alone microtubule, geometrically speaking, there are only two patterns of association sites and two more of dissociation sites; the rate constants for all of these four basic patterns can be found in Table 1. However, when the bead is on the microtubule, in addition to these patterns, there are five new patterns of association sites and another five new patterns of dissociation sites, as shown in Figs. 4 and 5. We need the rate constant that corresponds to each of these patterns in our model.

The method we will use is to explore the geometric similarities between different patterns and try to decompose the complicated new patterns into simpler patterns whose corresponding rate constants can be found directly from the four basic patterns shown Fig. 3. Furthermore, we assume that for association events, fewer molecules surrounding a site will lead to a smaller rate constant; for dissociation events, fewer molecules surrounding a site will lead to a larger rate constant.

Take the fourth pattern in Fig. 4, for example. It is geometrically similar to the second pattern in Fig. 3, so we assume that the rate constants are the same for these two patterns.

The first pattern in Fig. 4 is a case where we can apply the geometric decomposition method. According to the assumptions we made above, the rate constant for an association event in this case should be greater than that for the fourth pattern in Fig. 4 or the second pattern in Fig. 3. Therefore, we simply use the sum of the rate constants for these two simpler patterns as the rate constant for this pattern, as shown in case 1 of Fig. 6.

A more complicated example is the first pattern in Fig. 5. Here the outgoing molecule has direct contact with only one molecule in the microtubule, according to the assumptions we made above; the dissociation rate constant in this case is larger than that for the pattern when a molecule is at the corner of two molecules, such as the fourth pattern in Fig. 3. Therefore, we simply use the sum of the rate constant for the fourth pattern in Fig. 3, and that for the fourth pattern in Fig. 5, as the rate constant for this case. This is shown as case 3

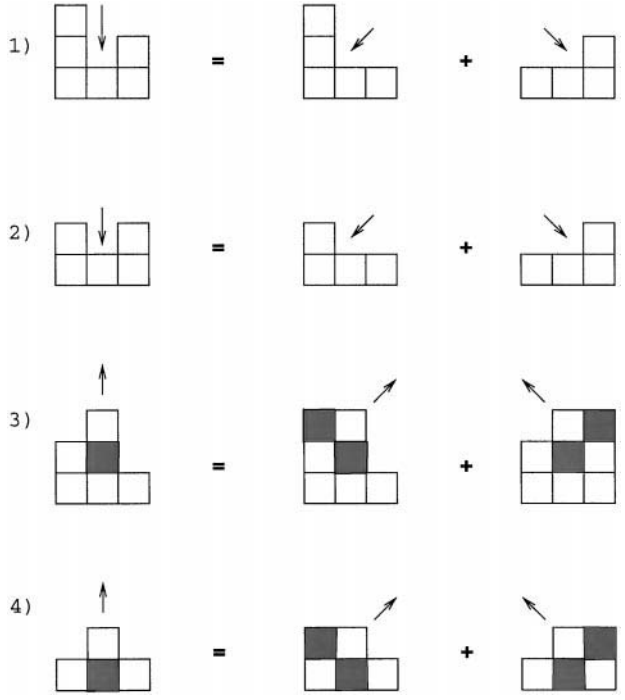

FIGURE 6 Calculating the rate constants for complex terminal configurations by decomposing them into simpler patterns whose corresponding rate constants are known. In each case, shaded units are occupied by the same kind of molecules (tubulin-GTP or tubulin-GDP).

in Fig. 6. Notice that in Fig. 6 certain units are shaded, which means that they are occupied by the same kind of molecules (tubulin-GTP or tubulin-GDP).

Similarly, the rate constants for all other patterns can be obtained either by exploring their geometric similarity with the known patterns or by decomposing them into the simpler patterns. As one can see, in the presence of the bead there are seven possible patterns of association sites and seven possible patterns of dissociation sites. For each pattern the rate constant is dependent on the contents of unit *b* and unit *d*, and in the case of a dissociation event, whether the outgoing molecule is tubulin-GTP or tubulin-GDP. This results in a much larger set of rate constants than the set for a stand-alone microtubule.

RESULTS AND DISCUSSION

Force-velocity curve

The relationship between the plus end-directed force and the velocity of the bead toward the minus end is calculated. The force-velocity curves corresponding to two different motor proteins, NK350 and kinesin, are shown by the two solid curves in Fig. 7. According to the present model, the difference in force-velocity curves of different motor proteins is due to the difference in p_{off}, i.e., the probability for the bead to pull off the molecule at the plus end of the protofilament along which it is moving. In this paper we use the same values of p_{off} as in Peskin and Oster (1995), where NK350 supposedly has a bigger p_{off} than kinesin. For both curves the concentration of tubulin-GTP in the environment is zero, which according to the model means that the microtubule can only depolymerize.

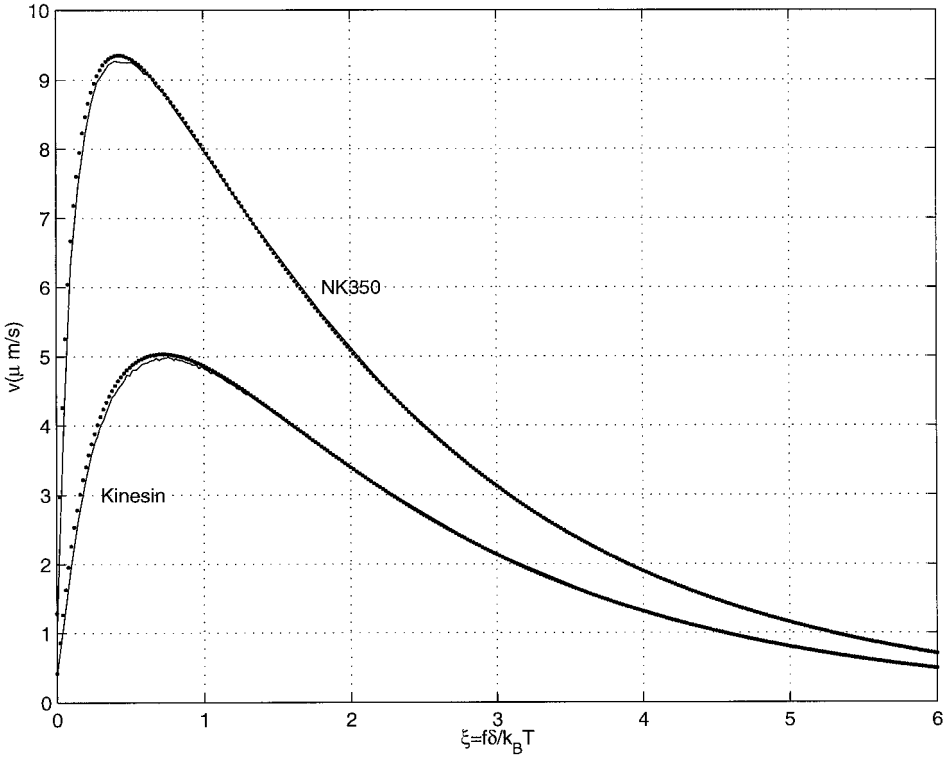

FIGURE 7 Force velocity curves at zero tubulin-GTP concentration. The solid lines indicate the force-velocity for two motor proteins, NK350 and kinesin, calculated using the present model. The dotted curves are calculated using the model in Peskin and Oster (1995). Notice that the force-velocity curves given by the two models are almost identical except for some difference at small load.

Each of these force-velocity curves has a maximum velocity, v_{max}, corresponding to a load f_1. When the force is less than f_1, an increase in the plus end-directed force actually speeds up the minus end-directed motion of bead. This has been observed in experiments as the paradoxical phenomenon that we described before: the addition of ATP to the environment, which fuels the plus motor protein, results in an increase in the velocity toward the minus end. Moreover, for the same load in our simulations, the bead travels faster when p_{off} is bigger, a bead coated with NK350 travels faster than one coated with kinesin.

When the force is greater than f_1, an increase in the plus end-directed force acting on the bead will start to slow down the motion of the bead toward the minus end. As the force increases, the velocity of the bead decreases very fast. For example, for NK350, corresponding to $\xi = 7.8$, or $f = 4$ pN, the velocity is only ~3% of the peak velocity. According to the lateral cap model, when the concentration of tubulin-GTP is zero the microtubule will be depolymerizing all the time; therefore, the force-velocity curve will never fall below the axis $v = 0$. When concentration of tubulin-GTP is not zero, however, the model does allow the velocity v to be less than zero, as we discuss later.

To get a smooth force-velocity curve from the Monte Carlo simulations, we calculated the velocity corresponding to each different force 50 times using different sequences of random number, and use the average velocity of these 50 runs in the force-velocity curve.

In Fig. 7 a comparison is made with the force-velocity curves given by the model of Peskin and Oster (1995), which are given by the dotted lines and described by the following equation:

$$v = \frac{(\delta\Gamma - v_{act})(\beta\delta + p_{off}v_{act})}{\delta[2\beta + \Gamma(1 - p_{off})] + v_{act}(1 + p_{off})}, \qquad (10)$$

where v is the velocity toward the minus end, $\Gamma = \gamma_+ + \gamma_-$, $v_{act} = \delta(\gamma_+ - \gamma_-)$, and β is the average depolymerization rate (in dimers/s) of a stand-alone microtubule that has no bead attached to it. Notice that β is a constant in the model of Peskin and Oster (1995); however, in the model presented in this paper, the depolymerization rate of the microtubule is no longer a constant. To make the comparison we first simulated a stand-alone microtubule at zero tubulin-GTP concentration and calculated the average depolymerization rate, which is accepted as β in Eq. 10.

One can notice in Fig. 7 that there is no significant difference between the force velocity curves given by the two models. The only noticeable difference (although still very small) is found at small load. This closeness is striking, considering the fact that in the model of Peskin and Oster (1995), a whole ring of 13 tubulin dimers comes together off the microtubule; therefore, each of the 13 protofilaments always has the same length. In the present model, individual tubulin molecules dissociate one by one, and there could be a very big discrepancy between the length of the protofilament along which the bead is moving and those of the other protofilaments. The fact that the force-velocity curves obtained from these two models are almost identical when the force is relatively large can be explained as follows: when the force is large (much greater than f_1), the bead is held at the end of the protofilament most of the time, and the movement of the bead toward the minus end is greatly hampered. Under such a condition there would not be too much difference between the length of individual protofilaments; hence the assumption that when the microtubule depolymerizes, a whole ring of 13 molecules comes off is very close to the real picture. However, even at small load, the difference in the force-velocity curves given by the two models is perhaps still too small to be differentiated in experiments. One could possibly argue that the force-velocity relationship is insensitive to the exact geometry of the end. Also, one should note that the force-velocity curve and the corresponding maximum velocity are remarkably different for kinesin and NK350. This suggests that it is possible to determine p_{off} by observing the force-velocity curve.

Run and pause

Fig. 8 shows one of the simulated trajectories of the bead obtained from the model. Fig. 8, *a* and *b* correspond to two different simulations for NK350 using different sequences of random numbers, *c* and *d* correspond to kinesin, and both are at zero load. Run and pause behavior is evident for NK350, as observed in experiments. The most rugged curve gives the trajectory of the bead, the uppermost curve gives the position of the tip of the protofilament along which the bead is moving, and the other curve gives the average position of the other 12 protofilaments. One conclusion that can be drawn from this figure is that run occurs when the bead is near the tip, while pause takes place when the bead departs away from the tip. This observation can be explained as follows: at zero load, the rate constants for the bead to move toward either end of the microtubule are the same; therefore, if the bead is not near the tip, on average the bead will be standing still, i.e., in the pause phase. Alternatively, when the bead is at the terminal unit, it could pull the terminal tubulin molecule off the protofilament, thus catalyzing the depolymerization of that protofilament. Note that after this happens the bead is still at the (new) end of the protofilament, so the process could be repeated, and the bead enters the run phase. In each of the subplots of Fig. 8, the uppermost line gives the average position of the tips of the other 12 protofilaments that the bead is not on. As one can see, for NK350 the tip of the protofilament along which the bead moves could be far away from the tips of the other protofilaments most of the time, suggesting that this protofilament depolymerizes much faster than the others. However, when the bead is in the pause phase, it is possible for the other protofilaments to catch up with the one that the bead is on; this is because when that protofilament is much shorter than the other protofilaments, the chance for a dis-

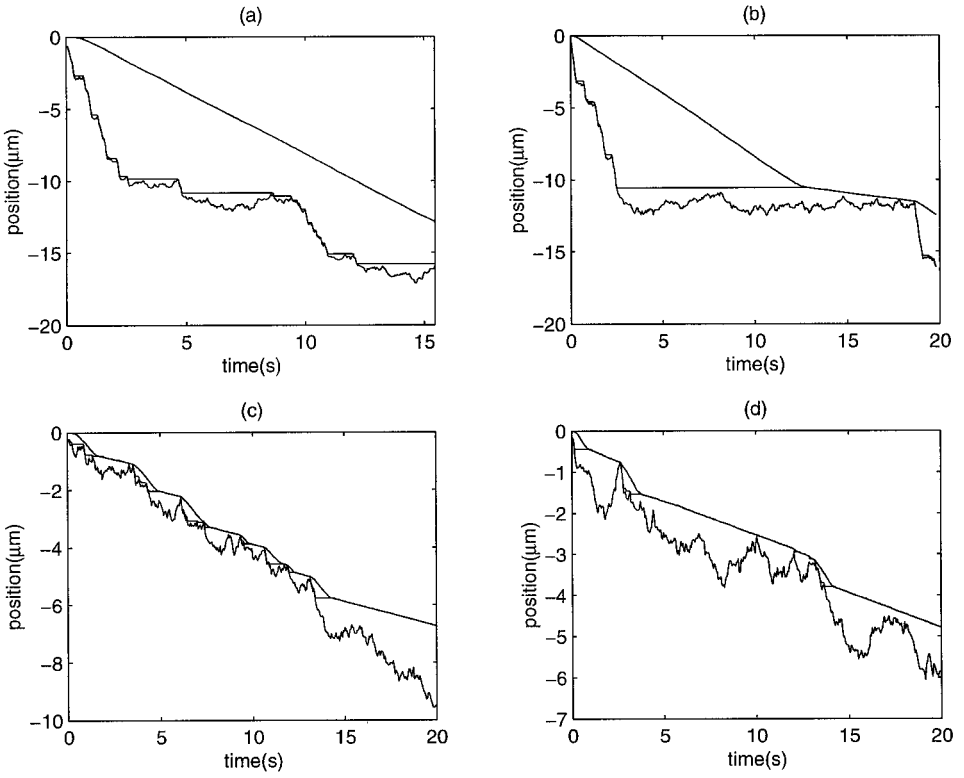

FIGURE 8 Run and pause. Both the load and the concentration of tubulin-GTP are zero. The most rugged curve shows the position of the bead, the uppermost curve shows the average position of the other 12 protofilaments, and the other curve shows the position of the tip of the protofilament on which the bead moves. (*a*) and (*b*) are the simulation results for NK350 (using different seeds for the random number generator), (*c*) and (*d*) are for kinesin. Notice that run and pause is much more evident for NK350 than for kinesin.

sociation site being selected at the end of that protofilament is almost zero according to the criteria that we have set before.

For kinesin, which supposedly has a lower p_{off} than NK350, run and pause is not so evident, as shown in *c* and *d* of Fig. 8. Furthermore, there is not much difference between the length of the protofilament along which the bead is moving and those of the other protofilaments.

It is important to point out that the parameter p_{off} is critical in determining the role that the bead plays in the system. One extreme case is when $p_{\text{off}} = 0$; in that case, we would expect that the behavior of the system will not differ too much from that of a stand-alone microtubule. For kinesin, which has a small p_{off}, run and pause is not so evident, and there is not much discrepancy between the length of the protofilament along which the bead is moving and those of the other protofilaments. p_{off} is dependent on the affinity of the tubulin molecules for the bead, or more precisely, for the motor protein that is coated on the bead. Therefore, distinct motor proteins will lead to different dynamics of transport.

The time scale of the run and pause for NK350 as shown in Fig. 8 is consistent with that observed in experiments (Lombillo et al., 1995). Furthermore, by measuring the time scale for run and pause and noticing the difference between the length of the protofilament along which the bead is moving and those of the other protofilaments, one can also make a rough estimate of the important parameter p_{off}.

In summary, the condition for the protofilament that the bead is on to depolymerize is either the bead at the tip of the protofilament, when the bead could pull the terminal molecule off the protofilament, or the length of that protofilament is very close to those of the other protofilaments, when it depolymerizes in a similar fashion as the other protofilaments.

Transport along a polymerizing microtubule

One of the new features of our present model in comparison with the previous model of Peskin and Oster (1995) is that in the present model, the microtubule could be polymerizing. Fig. 9 shows the simulated trajectory for NK350 when the concentration of tubulin-GTP is 5 μM. At this low level of tubulin-GTP concentration one can still find the run and pause characteristics in the trajectory. When the concentration of tubulin-GTP is at a much higher value, such as 20 μM, the protofilaments are polymerizing very fast, and the chance for the bead to catch up with the plus end of the protofilament is small; therefore, there is no longer any sign of run and pause in the trajectory of the bead.

For the force-velocity curve, when the concentration of tubulin-GTP is zero, the bead can move only toward the minus end; therefore, the velocity of the minus end-directed motion can never be less than zero. This is no longer the case when the concentration of tubulin-GTP is not zero, when the protofilaments could be polymerizing and it is possible for the bead to move toward the plus end. The force that corresponds to zero velocity is defined as the "stalling force." The force-velocity curve shown in Fig. 10 corresponds to NK350 at tubulin-GTP concentration of 20 μM, the calculated stalling force in this case is 4.8 pN. Of course, this only gives a rough estimate of the stalling force, be-

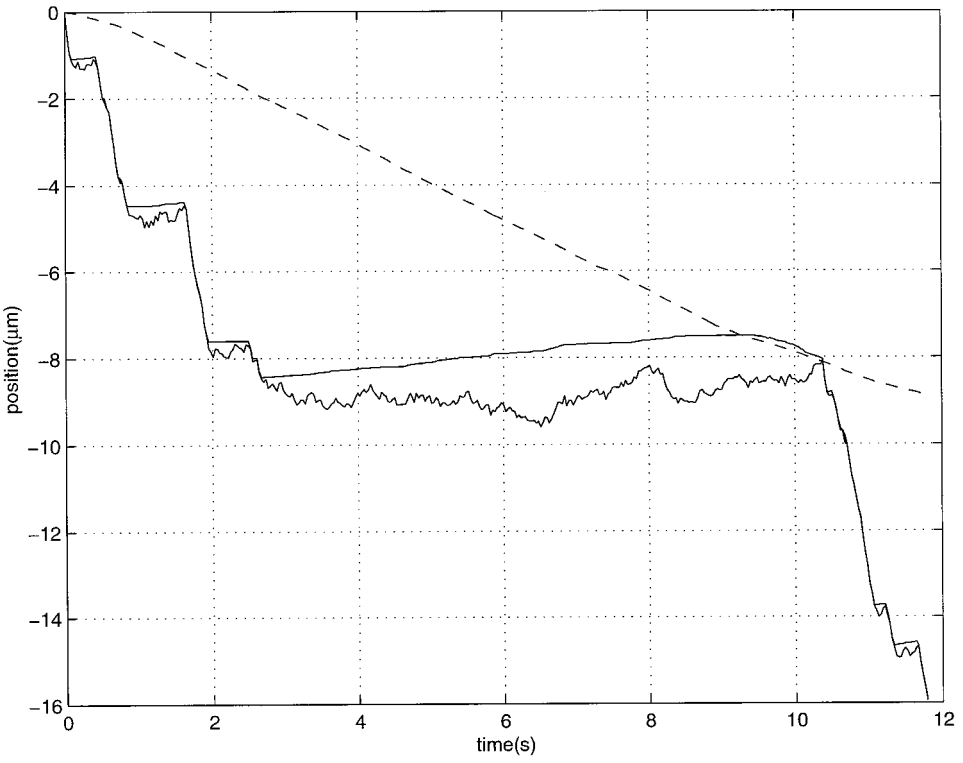

FIGURE 9 The trajectory of a bead coated with NK350 at zero load, when [Tu-GTP], the concentration of tubulin-GTP, is not zero, but still at a low level (5 μM). One can still find the run and pause characteristics, but the protofilament can grow sometimes.

cause as we mentioned before, when the force is large, the assumption that the bead will not fall off the microtubule when it is at the plus end might not be valid any more. There are no experimental data available for this situation. In comparison with the movement toward the minus end, the velocity of the bead toward the plus end is very small. This indicates that the primary role of microtubules in this case is to facilitate the transport toward the minus end.

Non-zero load

The trajectories of the bead shown above are obtained when the load is zero. When the load is not zero, simulated results show that the protofilament along which the bead is moving could depolymerize extremely fast in relation to the other protofilaments. Obviously, the role of the bead in catalyzing depolymerization is directly dependent on p_{off}, which is

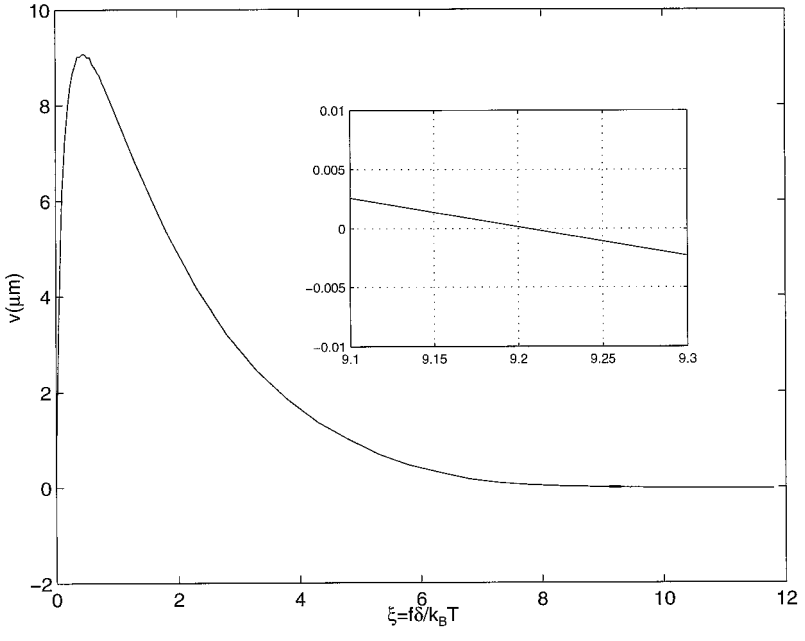

FIGURE 10 Force-velocity curve when the concentration of tubulin-GTP is not zero. Here [Tu-GTP] = 20 μM. Unlike the case when the concentration of tubulin-GTP is zero, here the force-velocity curve crosses the axis $v = 0$, as shown in detail in the inset. The force corresponding to $v = 0$ is the stalling force. Notice that when the force is larger than the stalling force, the velocity toward the plus end is extremely small in comparison with the velocity toward the minus end when the force is much smaller than the stalling force.

determined by the affinity of the motor protein for the tubulin molecules.

For any motor protein having a certain value of p_{off} the depolymerization rates at different loads are also different. At low loads, an increase in load causes the microtubule to depolymerize faster. This is because a larger plus end-directed force keeps the bead near the plus end, where catalysis due to the bead is most effective. Recall, however, that this catalyzing effect depends on the motion of the bead away from the plus end. At high loads the bead is held so tightly to the plus end of the protofilament that it actually stabilizes the protofilament by preventing the depolymerization of the terminal unit. Of course, how strong the load (plus end-directed force) can be before the detachment of the bead from the microtubule takes place is something yet to be determined by experiments.

Experiments suggested by the model

With the advent of new experimental techniques such as laser trapping (Svoboda et al., 1993; Coppin et al., 1997), it is possible to apply a specific load to the bead. Previously, different "loads" were obtained by using an active motor and varying the ATP concentration. This resembles the application of a load force since the activity of the motor biases the random walk of the bead toward the plus end of the microtubule, but the interpretation of that is complicated by not knowing the dynamics of the motor in detail. As a result, it is difficult to determine quantitatively the exact load. So it would be more clearcut to use a passive motor (i.e., one that is not functioning as a motor), and to subject the bead to a known force with a laser trap.

The model makes specific predictions of several things as functions of the applied load, namely 1) the mean velocity of the bead, 2) the time scale and statistics of runs and pauses, and 3) the statistics of the average length of the other protofilaments beside the one that the bead is on. All of them can be measured in experiments.

Furthermore, the model is able to simulate the situation in which the concentration of GTP-tubulin is not zero, so it predicts all of the above not only as a function of the applied force, but also as a function of the concentration of GTP-tubulin.

Experiments could be done for different (passive) motor proteins linking the bead to the microtubule. By changing the parameter p_{off} in the model and fixing the other parameters, one should be able to simulate the behavior of several different motor proteins.

One way to test the validity of the model is to use the model together with part of the experimental data to calculate the value of p_{off} of a particular motor protein and then to use the model to predict the rest of the data for that motor protein by setting the value of p_{off} in the model to the one we just obtained.

One approach would be to use the force-velocity curve to determine p_{off}. As one can see from Fig. 7, for different motor proteins that have different p_{off}, the force velocity curves are different. One way to tell p_{off} from the force-velocity curve is to measure the maximum velocity the bead. As we can see, corresponding to different values of p_{off}, the maximum velocities as given by the simulated force-velocity curves are different. However, the model also predicts that run and pause behavior could be noticeably different for different motor proteins. this corresponds to different values of p_{off} in the model.

Therefore, with p_{off} obtained from the first approach, i.e., the measurement of the force-velocity curve, one can simulate the run and pause statistics using the model. The time scale and statistics of such behavior given by the simulation should be consistent with what is observed in experiments.

An interesting new feature of the present model in comparison to the one of Peskin and Oster (1995) is its capability to simulate the situation when the concentration of GTP-tubulin is greater than zero. Few experimental data are available in this realm. But as the model predicts, one can still notice the run and pause behavior at relatively small concentration of GTP-tubulin. At high concentration, however, there will be little chance for the bead to catch up with the end of the microtubule and, therefore, run and pause behavior would no longer be evident. Experiments can be performed to verify these results and test the validity of the model.

By repeating this procedure for several different motor proteins, one would considerably sharpen the test of the model. Note that most of the parameters of the model are independent of the motor protein and can be found from experiments on a stand-alone microtubule. The rate constant γ that characterizes the random walk of the bead on the microtubule may depend on the motor protein, but it can be directly measured by observing the random walk of the bead on a stabilized microtubule (one that is neither polymerizing nor depolymerizing). Thus p_{off} is the only parameter that has to be determined by curve-fitting, and it should be possible to fit the data for a whole variety of motor proteins with all model parameters constant except for γ and p_{off}.

Yet another test of the model would be to vary the size of the bead, which would be expected to change γ (in a measurable way, as above) and possibly p_{off}. Again, the test would be to predict a whole family of data for beads of different sizes while changing only those two parameters.

CONCLUSIONS

In this paper we have presented a numerical model that can simulate a system consisting of a microtubule and a latex bead coated with motor protein. Substantial generalizations are made to the lateral cap model to accommodate the new terminal configurations due to the movement of the bead along the microtubule. The rate constants for association and dissociation of tubulin molecules at these new terminal configurations are obtained by exploring the geometric similarities and by decomposing new terminal patterns into simpler patterns whose rate constants are known.

When the concentration of tubulin-GTP in the environment is zero, the force-velocity curve calculated with the present model bears a striking resemblance to the one obtained with the model presented by Peskin and Oster (1995). Unlike their model, the present model can also be used to calculate the force-velocity curve for the case when the concentration of tubulin-GTP is not zero. An experimental result for this situation does not seem to exist so far. A stalling force, at which the bead start to reverse its direction of movement, is calculated. When the force acting on the bead is greater than the stalling force, on the average the bead moves (very slowly) toward the plus end of the microtubule, but the exact stalling force might be difficult to determine in experiments because the slope of the force-velocity curve is close to zero near the stalling force.

Determining the force-velocity curve can give valuable information about the system. For example, the force-velocity curve and the corresponding maximum velocity are different for different motor proteins. It is therefore possible to determine p_{off} from the force-velocity curve.

In comparison with the maximum velocity toward the minus end, the velocity toward the plus end is extremely small, even if the force acting of the bead is relatively large. This suggests that for this mechanism of transport, the role of the microtubule is more disposed to fast minus end-directed transport.

The coupling between the bead and the microtubule, which is dependent on the affinity of the motor protein for the tubulin molecule, is reflected in the present model by the probability that the bead can pull off a terminal molecule at the plus end of the protofilament, i.e., p_{off}. In essence, p_{off} determines the extent to which the bead can affect the dynamics of the system.

When p_{off} is close to unity, which indicates a strong affinity between the motor protein and the tubulin molecule, and the concentration of tubulin-GTP is relatively small, the trajectory of the bead has the run and pause characteristics at zero load. However, if the load is not zero, the depolymerization rate of the protofilament along which the bead is moving is extremely large, as a result of the bead catalyzing the depolymerization of the protofilament. When p_{off} is close to zero, however, the role of the bead in influencing the dynamics of the system is very limited. This might explain the difference of various motor proteins in affecting intracellular transport driven by the depolymerization of microtubules.

The time scale of run and pause of the simulated trajectory for a bead coated with NK350 is consistent with experimental evidence. For kinesin, the simulated trajectory given by the model indicates that run and pause is no longer evident. Once p_{off} has been determined from the force-velocity curve, it can be used to predict the statistics of the time scale of run and pause, thus providing a strong check on the model.

The authors thank George Oster for his help and valuable suggestions.

This work was supported in part by National Science Foundation Grant FD92-20719.

REFERENCES

Alberts, B., D. Bray, J. Lewis, M. Raff, K. Roberts, and J. D. Watson. 1994. Molecular Biology of the Cell, Chap. 16. Garland Publishing, New York.

Bayley, P. M., M. J. Schilstra, and S. R. Martin. 1990. Microtubule dynamic instability: numerical simulation of microtubule transition properties using a lateral cap mode. *J. Cell Sci.* 95:33–48.

Coppin, C. M., D. W. Pierce, L. Hsu, and R. D. Vale. 1997. The load dependence of kinesin's mechanical cycle. *Proc. Natl. Acad. Sci. USA.* 94:8539–8544.

Coue, M., V. A. Lombillo, and J. R. McIntosh. 1991. Microtubule depolymerization promotes particle and chromosome movement in vitro, *J. Cell Biol.* 112:1165–1175.

Desai, A., and T. J. Mitchison. 1995. A new role for motor proteins as couplers to depolymerizing microtubules. *J. Cell Biol.* 128:1–4.

Dogterom, M., and S. Leibler. 1993. Physical aspects of the growth and regulation of microtubule structures. *Phys. Rev. Lett.* 70:1347–1350.

Hill, T. L. 1984. Introductory analysis of the GTP-cap phase-change kinetics at the end of a microtubule, *Proc. Natl. Acad. Sci. USA.* 81:6728–6732.

Hill, T. L., and Y. D. Chen. 1984. Phase changes at the end of a microtubule with a GTP cap. *Proc. Natl. Acad. Sci. USA.* 81:5772–5776.

Howard, J. 1995. The mechanics of force generation by kinesin. *Biophys. J.* 68:245S–255S.

Hyams, J. S., and C. W. Lloyd, editors. 1994. Microtubules. Wiley-Liss, New York.

Inoué, S. 1981. Cell division and the mitotic spindle. *J. Cell Biol.* 91: 131s–147s.

Koshland, D. E., T. J. Mitchison, and M. W. Kirschner. 1988. Poleward chromosome movement driven by microtubule depolymerization in vitro. *Nature.* 331:499–504.

Lombillo, V. A., R. J. Stewart, and J. R. McIntosh. 1995. Minus end-directed motion of kinesin-coated microspheres driven by microtubule depolymerization. *Nature.* 373:161–164.

Mandelkow, E. M., E. Mandelkow, and R. A. Milligan. 1991. Microtubule dynamics and microtubule caps: a time-resolved cryo-electron microscopy study. *J. Cell Biol.* 114:977–991.

Martin, S. R., M. J. Schilstra, and P. M. Bayley. 1993. Dynamic instability of microtubules: Monte Carlo simulation and application to different types of microtubule lattice. *Biophys. J.* 65:578–596.

Mitchison, T., and M. Kirschner. 1984. Dynamic instability of microtubule growth. *Nature.* 312:237–242.

Odde, D. J., L. Cassimeris, and H. M. Buettner. 1995. Kinetics of microtubule catastrophe assessed by probabilistic analysis. *Biophys. J.* 69: 796–802.

Peskin, C. S., and G. F. Oster. 1995. Force production by depolymerizing microtubules: load-velocity and run-pause statistics. *Biophys. J.* 69: 2268–2276.

Rieder, C. L., and S. P. Alexander. 1990. Kinetochores are transported poleward along a single astral microtubule during chromosome attachment to the spindle in newt lung cells. *J. Cell Biol.* 110:91–95.

Roberts, K., and J. S. Hyams, editors. 1979. Microtubules. Academic Press, New York.

Semënov, M. V. 1996. New concept of microtubule dynamics and microtubule motor movement and new model of chromosome movement in mitosis. *J. Theor. Biol.* 179:91–117.

Svoboda, K., C. F. Schmidt, B. J. Schnapp, and S. M. Block. 1993. Direct observation of kinesin stepping by optical trapping interferometry. *Nature.* 365:721–727.

Wade, R. H., and A. A. Hyman. 1997. Microtubule structure and dynamics. *Curr. Opin. Cell Biol.* 9:12–17.

Walker, R. A., E. T. O'Brien, N. K. Pryer, M. F. Soboeiro, W. A. Voter, and H. P. Erickson. 1988. Dynamic instability microtubules analyzed by video light microscopy: rate constants and transition frequencies, *J. Cell Biol.* 107:1437–1448.